Environ. Sci. Technol. **1998**, *32,* 2100−2105

Population Heterogeneity Affects Transport of Bacteria through Sand Columns at Low Flow Rates

STEFANO F. SIMONI,*,† HAUKE HARMS,† TOM N. P. BOSMA,‡ AND ALEXANDER J. B. ZEHNDER†

Swiss Federal Institute for Environmental Science and Technology (EAWAG) and Swiss Federal Institute of Technology (ETH), Überlandstrasse 133, CH-8600 Dübendorf, Switzerland, and TNO Institute of Environmental Sciences, P.O. Box 342, NL-7300 AH Apeldoorn, The Netherlands

Travel distances of bacteria in groundwater aquifers often exceed predictions based on filtration theories. These findings have mostly been ascribed to structural heterogeneities in the subsurface, but variations in the adhesive properties within the microbial populations have been observed too. In laboratory experiments with *Pseudomonas* sp. strain B13, we found that only a fraction of the cells was efficiently deposited in sand columns while the remainder passed a second column identical to the first without hindrance. Upon rinsing the columns with deionized water, between 10 and 35% of the deposited cells were flushed out, thus showing that increased electrostatic repulsion between sand and bacteria partially reverted the deposition. Lipopolysaccharides (LPS) extending from the cell surface into the medium as well as estimated DLVO-type interaction energy curves indicate that cells were trapped at a distance of more than 20 nm from the sand surface. We hypothesize that differences in the LPS coat were responsible for the fractionation of the bacterial population. Our results indicate that the high travel distances of microorganisms might be due not only to the complex structure of aquifer material but also to heterogeneity in the adhesion properties within the bacterial populations.

Introduction

The interest in the dissemination and deposition of microorganisms in the subsurface was initially based on obvious concerns about drinking water quality and spread of disease (*1*). The study of bacterial transport has been further motivated by the enhancement of contaminant transport by bacteria, their use for bioremediating polluted aquifers, and the potential spread of genetically engineered organisms (*2*). Whereas observations were discussed qualitatively in earlier reports (*3*−*5*), other authors introduced clean bed filtration theory (*6, 7*) and more elaborate kinetic models (*7, 8*) to describe deposition of bacteria. These concepts were developed further to include additional effects, such as the reduction of deposition by already adhered cells (*9, 10*), often referred to as blocking. Nevertheless, travel distances of several 100 m found for bacteria in aquifers exceeded predictions with experimentally determined filtration parameters by far (*6, 11*). These discrepancies were ascribed to heterogeneities in aquifers leading to preferential flow paths (*4, 6, 11*).

Variation of adhesive properties within a population of bacteria could also lead to similar observations although reports on this subject are scarce. Shales et al. (*5*) subjected the nonadherent bacteria from a batch adhesion assay to a second assay and found them to stick significantly less than controls. They postulated the existence of two subpopulations of bacteria. Albinger et al. (*12*) showed that, for those bacteria transported across the first centimeter of a column packed with glass beads, the probability to be captured became very small. Recently, Johnson and co-workers (*13*) described a dependence of cell detachment on residence time on the surface. To interpret their results, they developed a kinetic model ascribing different detachment rate constants to two subpopulations. Their observations are in qualitative agreement with data obtained with a flow chamber (*14*). However, the latter authors interpreted their results in terms of increasing bond strength with time. Both explanations were already mentioned by van de Ven (*15*): Either a distribution in bond strength—two coexisting subpopulations would be a simple case thereof—or a time dependence of bond strength would lead to nonexponential detachment.

In this paper, we present evidence for the significance of heterogeneity in microbial populations for the subsurface transport of bacteria. We percolated dilute suspensions of *Pseudomonas* sp. strain B13 through columns filled with purified sand at flow rates common in natural aquifers. The results are discussed in terms of a simple model accounting for two fractions with different adhesive properties. Characterization of the cell surface allowed us to develop a mechanistic interpretation based on energy interaction curves derived from the DLVO theory of colloid stability.

Materials and Methods

Organism and Culture Conditions. *Pseudomonas* sp. strain B13 (*16*) is able to utilize 3-chlorobenzoic acid (3-cba) as the sole source of carbon and energy. We grew the cells in a phosphate buffer containing minerals and trace elements that was amended with 5 mM 3-cba (*17*). After gaining maximal cell density, cells were kept in a carbon-limited state for approximately 16 h before harvest. We prepared cell suspensions by resuspending centrifuged bacteria to final densities between 2×10^7 and 4×10^8 cells mL^{-1}. To avoid partial removal of cell envelope constituents, we renounced on extra washing steps. Tros et al. (*17*) showed for similar conditions that the cells keep their metabolic activity for up to 48 h, thus indicating that they remain intact during this time period. Microscopic inspection showed that the resting cells were not motile although they move lively during growth. Electron micrographs after negative staining as well as tests for chemotaxis by a modified capillary assay according to Adler (*18*) suggest that flagella were absent in the starvation phase.

Electrolyte Chemistry. Electrolytes used for preparing cell suspensions and for equilibrating the columns were based on a 10-fold diluted growth medium in which phosphate was replaced by MOPS/NaOH buffer at pH = 7.2 and $(NH_4)_2SO_4$ was used instead of NH_4NO_3. This solution was brought to a total ionic strength of $I = 8$ mM with $MgSO_4$, which accounted for ∼65% of the final ionic strength. In the calculation of the ionic strength, we accounted for the formation of soluble and neutral $MgSO_4^0$ complexes at a concentration of $C \sim 0.5$ mM (*19*). All electrolytes were

* Corresponding author phone: ++ 41 1 823 55 16; fax: ++ 41 1 823 55 47; e-mail: stefano.simoni@eawag.ch.
† EAWAG and ETH.
‡ TNO Institute of Environmental Sciences.

S0013-936X(97)00936-X CCC: $15.00
Published on Web 05/30/1998

prepared with deionized water (Nanopure Cartridge System, SKAN, Basel, Switzerland).

Deposition Experiments. We conducted filtration experiments in glass columns (2.5 cm i.d., Omnifit, Cambridge, U.K.) with polyethylene frits (25 μm pore diameter) and one adjustable endpiece. The columns were packed wet with silica sand (Fluka, Buchs, Switzerland) consisting of cristobalite. We washed the sand with 1 mM HCl, rinsed it several times with 10 mM $NaNO_3$ to reach a pH close to neutrality, and dried it overnight at 80 °C. A total of 10, 50, and 90% of the grains (number based) were below 150, 238, and 345 μm in diameter, respectively, as measured by static light scattering (Master Sizer X, Malvern Instruments, Malvern, U.K.). We gravimetrically estimated the porosity ϵ in the columns to be 0.45. Columns were operated in downflow mode with a peristaltic pump (Ismatec, Glattbrugg, Switzerland) at Darcy velocities $0.6 < U < 9$ cm h^{-1}. Connecting tubings consisted of polyethylene and tygon (Ismatec, Glattbrugg, Switzerland). Filtration studies with bacterial suspensions were started after equilibrating the columns for at least 10 pore volumes (PV). We sampled the column outflow by aid of a fraction collector. Turbidity as a measure for cell density was determined photometrically at 280 nm after carefully shaking the sample vials. Absolute cell numbers were deduced after calibration to plate counts. The quantification of cells was possible down to less than 5×10^6 cells mL^{-1}. To characterize the flow conditions prevailing in our columns, we performed tracer tests in control experiments without cells by following the breakthrough of 1.0 mM KBr online at 220 nm with a Jasco 870-UV detector (Jasco, Tokyo, Japan).

Surface Characterization. (i) Electrophoretic Mobility and Surface Potential. Electrophoretic mobility u_E of bacteria suspended in the medium used for the column experiments ($I = 8$ mM) was measured by dynamic light scattering (Zetamaster, Malvern Instruments, Malvern, U.K.). Surface potentials were approximated by the ζ-potentials at the electrokinetic shear plane, which can be deduced from u_E by the Smoluchowsky relationship (*20*). To obtain estimates for the ζ-potential of sand, we ground sand particles in a mortar and determined u_E of the fraction remaining in suspension for several hours.

(ii) Contact Angles. Contact angles of water droplets on a bacterial lawn were determined as described by ref *21*.

(iii) Size Determination of Lipopolysaccharides (LPS) on the Cell Surface. We isolated, purified, and hydrolyzed LPS according to Jucker et al. (*22*). These authors give as well the method for the size determination of the O-antigens, which are the sugar chains of the LPS actually extending into the medium.

Electron Micrographs. Bacteria were cryofixed by propane jet freezing (*23*) and freeze substituted in acetone containing 2% osmium tetroxide. The frozen samples were kept at −90, −60, and −30 °C for 8 h each and finally brought to 0 °C in a cryostage (*24*). After the samples were washed three times in acetone, they were embedded in Epon. The sections were stained with uranyl acetate and lead citrate (*25*). Pictures were taken with a Philips EM 301 (Philips Electron Optics, Eindhoven, The Netherlands).

Filtration Model. Although deposition of bacteria must be assumed to be reversible in principle (*7*, *8*, *14*), assuming irreversible removal might be useful for describing the initial stage of deposition where low surface coverages prevail. Various authors (*6*, *7*) applied clean bed filtration theory (*11*, *26*) to irreversible first-order removal of bacteria in sand columns at low surface coverages according to

$$C = C_0 \exp\left(-\frac{3}{4}\frac{(1-\epsilon)}{r_c}\eta\alpha L\right) = C_0 \exp(-\alpha\lambda L) \quad (1)$$

where C is the effluent cell concentration, C_0 is the influent cell concentration, ϵ is the porosity of the packed bed, r_c is the radius of the collector sand grain, L is the length of the flow path, η is the single collector efficiency, and α is the collision efficiency. Equation 1 is often simplified by defining a filtration coefficient λ. η describes the transport of particles from the bulk solution to the collector surface and can be theoretically derived from approximate solutions to the convective−diffusion equation (*26*, *27*). The calculations of η include diffusion, interception, and settling as deposition mechanisms and are based on the parameters given in Table 1. In the flow-velocity range we used, η is mainly determined by diffusion, leading roughly to a dependency on the Darcy velocity U according to

$$\eta \propto U^{-2/3} \quad (2)$$

indicating that the filtration coefficient λ increases with decreasing U. The collision efficiency α gives the fraction of collisions effectively, resulting in attachment of the particle and reaches 1 in the absence of repulsive forces. A simple way to account for heterogeneous deposition within a population of bacteria is to postulate two subpopulations of cells with different collision efficiencies α_{fast} and α_{slow}:

$$C = C_0(f_{fast}\exp(-\alpha_{fast}\lambda L) + f_{slow}\exp(-\alpha_{slow}\lambda L)) \quad (3)$$

with

$$f_{fast} + f_{slow} = 1$$

where f_{fast} and f_{slow} denote the fractions of the population undergoing fast and slow removal, respectively.

Estimation of Interaction Energy According to the DLVO Theory of Colloid Stability. Although live bacteria are more complex than abiotic colloids, they can basically be regarded to follow the principles of colloid chemistry (*33*). The interaction energy $\Delta G^{DLVO}(h)$ between a cell (radius r_p) and a flat plate (collector with radius r_c and $r_p \ll r_c$) was estimated as described by Elimelech and O'Melia (*31*) except that besides the terms accounting for retarded Lifshitz−van der Waals attractions (ΔG^{LW}) and electrostatic interactions (ΔG^{EL}) incorporation of a third term arising from acid−base type interactions (ΔG^{AB}) was considered (*32*). For reasons given below, we confined our calculations to the region beyond the energy barrier resulting from electrostatic repulsion (secondary minimum of ΔG^{DLVO}). Our calculations of $\Delta G^{DLVO}(h)$ were based on the parameters in Table 1. Similar to Meinders et al. (*14*), we found that we could neglect ΔG^{AB} under these conditions. Note that the use of a term for retarded Lifshitz−van der Waals forces results in less pronounced secondary minima than those obtained with the unretarded term for ΔG^{LW} and sphere-plate geometry (*14*, *30*).

Results and Discussion

Deposition and Release of *Pseudomonas* sp. B13 in Sand Columns. Dilute suspensions of *Pseudomonas* sp. strain B13 were percolated through sand columns of a length $L = 3.1$ cm at Darcy velocities $1.2 < U < 1.3$ cm h^{-1}. The fairly low Peclet numbers $Pe = LU/(\epsilon D_{disp})$ we deduced from tracer experiments with KBr ($8 < Pe < 15$) show the importance of dispersion processes. These lead to smooth curvatures at the edges of the input steps but do not affect the breakthrough level (Figure 1). Plots of relative cell densities in the column outflow (C/C_0) against time normalized to the number of pore volumes exchanged (t^*) showed an incomplete and unretarded initial breakthrough of cells after $t^* = 1$ PV followed by a leveling off for $t^* > 2$ PV (Figure 1). Usually the plateau after the initial breakthrough was nearly horizontal, although both a slight increase or decrease of C/C_0 with time were observed occasionally. Confidence intervals of C/C_0 reached 0.07 for $n = 23$ (Figure 2). Upon flushing

TABLE 1. Parameters Used for Calculation of Collector Efficiency η and Interaction Energy ΔG^{DLVO}

	parameter			source
r_c	sand grain/collector radius[b]	(m)	1.3×10^{-4}	*a*
r_p	cell/particle radius	(m)	5.0×10^{-7}	*28*
ϵ	porosity	(−)	0.45	*a*
μ	water viscosity	(kg m^{-1} s^{-1})	1.0×10^{-3}	
ρ_p	cell density	(kg m^{-3})	1.1×10^{3}	*29*
ρ_w	water density	(kg m^{-3})	1.0×10^{3}	
D_p	diffusion coefficient for cells	(m^2 s^{-1})	4.3×10^{-13}	*28*
I	ionic strength	(M)	8×10^{-3}	*a*
U	Darcy velocity	(m s^{-1})	3.4×10^{-6}	*a*
g	gravitational acceleration	(m kg s^{-2})	9.81	
k	Boltzmann constant	(J K^{-1})	1.38×10^{-23}	
T	temperature	(K)	295	
A_{pwc}	Hamaker constant cell-water-glass	(J)	7.0×10^{-21}	*30*
ζ_p	ζ-potential of cells	(V)	-23×10^{-3}	*a*
ζ_c	ζ-potential of sand	(V)	-37×10^{-3}	*a*
ϵ_r	dielectric constant	(−)	78	
ϵ_0	permittivity of the vacuum	(C^2 J^{-1} m^{-1})	8.85×10^{-12}	
λ^{LW}	decay length for retarded Lifshitz−van der Waals interactions	(m)	1.0×10^{-7}	*31*
θ	water contact angle	(deg)	32	*28*
λ^{AB}	decay length for acid−base interactions	(m)	1.0×10^{-9}	*32*
h_0	distance of closest approach for acid−base interactions	(m)	1.6×10^{-10}	*32*

[a] This study. [b] Number-based mean.

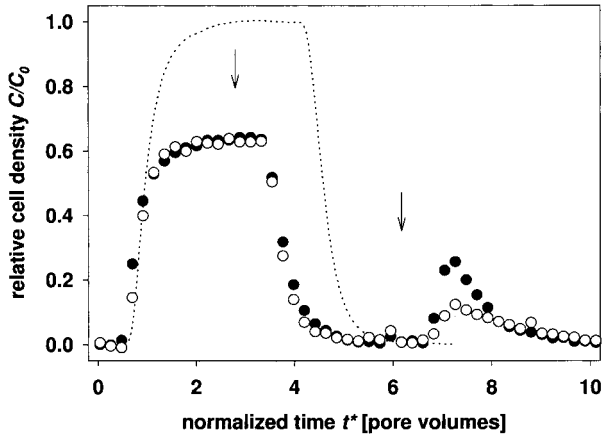

FIGURE 1. Relative cell density C/C_0 in the outlet of sand columns as a function of normalized time t^* showing breakthrough and washout ($L = 3.1$ cm, $U = 1.2$ cm h^{-1}). Cells suspended in buffers amended with $MgSO_4$ ($I_{tot} = 8$ mM) were pumped through replicate columns. After 2.8 pore volumes (arrow on the left), the influent solution was replaced by a cell-free buffer of the same composition. A switch in the column feed to deionized water after 6.2 pore volumes (arrow on the right) resulted in a washout of 10−35% of the deposited cells (●, data from a representative experiment are shown). Washout was not enhanced when a buffer of lower ionic strength containing Na_2SO_4 in place of $MgSO_4$ was used instead (○, $I_{tot} = 1$ mM). This indicates that exchange of Mg^{2+} by Na^+ was not of great importance for the system. A representative tracer curve obtained by following the breakthrough of 1.0 mM KBr online is shown for comparison (- -, pulse duration = 3.3 pore volumes).

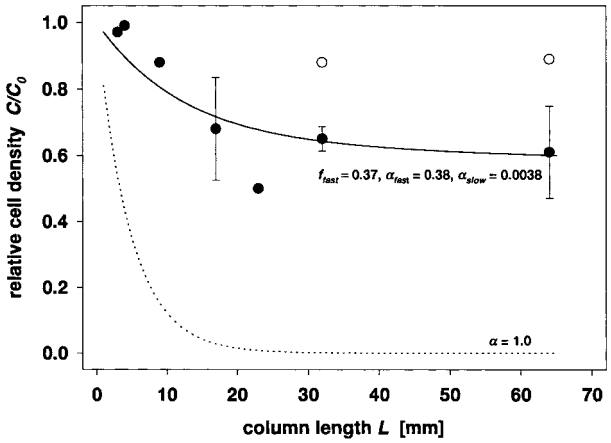

FIGURE 2. Relative cell density C/C_0 in the column outlet after initial breakthrough as a function of column length L (●) for 1.2 cm h^{-1} < U < 1.3 cm h^{-1} and $I = 8$ mM. For the points at 17, 32, and 64 mm, the 95% confidence interval is given ($n = 5$, 23, and 6, respectively). A curve obtained by fitting eq 3 to the data points is shown (—). Datapoints obtained with columns connected to the outflow of a second identical column (○) show that the overall collision efficiency α varies within the population. A curve describing favorable deposition according to colloid filtration theory is given for comparison (- -, $\lambda = 278$ m^{-1}, parameters given in Table 1).

the columns with cell-free solutions of identical chemical composition, we only found slight tailing during the washout. The above findings indicate that detachment is negligible under these conditions and that first-order removal of cells governs deposition. This seems reasonable since the estimated maximal surface coverage remained below 1.3%. However, after changing the inflow to deionized water, 10−35% of the deposited cells were flushed out of the columns (Figure 1). This shows that the deposition was partially reverted by the increased electrostatic repulsion between sand and bacteria (*30*, *34*) resulting from the lowered ionic strength (*20*). In contrast to other studies (*35*), percolation with a buffer of $I = 1.0$ mM amended with Na_2SO_4 instead of $MgSO_4$ did not enhance the release of cells (Figure 1). We therefore concluded that exchange of bivalent Mg^{2+} with monovalent Na^+ was not critical for reversibility.

Effect of Column Length L on C/C_0 in the Outflow. In contrast to eq 1, levels of C/C_0 after initial breakthrough decreased very slowly once column length exceeded 3 cm (Figure 2). Further experiments confirmed that almost all

TABLE 2. Comparison of Cell Properties before and after Column Passage of *Pseudomonas* sp. Strain B13 (I = 8 mM)

cell property		before	after
electrophoretic mobility[a]	(10^{-8} m^2 V^{-1} s^{-1})	−1.9 (0.2)	−2.1
contact angles[a]	(deg)	32 (5)	[25−][b] 30
length[c]	(μm)	1.50 (0.08)	1.39 (0.07)
width[c]	(μm)	1.08 (0.04)	0.89 (0.03)

[a] Means from two independent experiments are given. Values in parentheses give measurement precision derived from larger series. [b] In one experiment, data after column passage were unreliable due to the low amount of cells available. [c] Data from a single experiment where 40 cells in the inflow and 80 cells in the outflow were measured on photomicrographs. The 95% confidence interval is given in parentheses.

the cells that were not retained in a first column passed a second identical column without hindrance (Figure 2), a finding that can be understood only by assuming that the collision efficiency α is not the same for all the bacteria in the initial suspension. The fraction of cells depositing fast according to eq 3 was estimated at $f_{fast} = 0.36 \pm 0.048$ and the respective collision efficiency at $\alpha_{fast} = 0.32 \pm 0.15$ by least-squares fitting. To obtain reasonable agreement with our observations, α_{slow} had to be fixed below $10^{-2} \times \alpha_{fast}$. More complicated models tested for adequacy to describe the variability of α (normal distribution, log-normal distribution) did not improve agreement with the experimental findings (data not shown). Cells leaving the sand columns fractionated again in the same manner when regrown on fresh medium, thus suggesting that differences in genotype were not responsible for the heterogeneity within the bacterial culture. To test whether bacterial excretions gradually modified the collector surface during column passage (*36*), we pretreated sand columns with the supernatant of centrifuged cell suspensions. Deposition in the pretreated columns, however, remained the same as in untreated controls. As cell size and shape were expected to be critical factors for bacterial deposition (*37*, *38*), we compared length and width of cells in the outflow and in the inflow of a column (Table 2). Although cells in the outflow tended to be slightly smaller, the expected change in the deposition rate was unimportant. Differences in contact angles or ζ-potentials between cells in the outflow and those in the feed were small as compared to the measurement precision (Table 2) and therefore considered insignificant.

Consequences for the Calculation of the Collision Efficiency α. When our findings based on eq 3 are interpreted with a single α for the whole population, they result in a dependency of α on the filtration path length L (Figure 3). This dependency can be expressed as a local $\alpha_{local}(L)$ derived from the slope of C/C_0 vs L. Upon equating the first derivatives with respect to L of eqs 1 and 3, substituting for C from eq 3 and solving for α, we obtain

$$\alpha_{local}(L) = \frac{f_{fast}\exp(-\alpha_{fast}\lambda L)\alpha_{fast} + f_{slow}\exp(-\alpha_{slow}\lambda L)\alpha_{slow}}{f_{fast}\exp(-\alpha_{fast}\lambda L) + f_{slow}\exp(-\alpha_{slow}\lambda L)} \quad (4)$$

This approach underlines the agreement of our findings with published data obtained from the biomass distribution in columns filled with glass beads (*12*). More often, however, average collision efficiencies $\alpha_{average}$ up to filtration distance L are reported without (*39*−*41*) or only with scarce (*7*) information on variability with L. In our case, $\alpha_{average}$ can be calculated by equating the logarithms of eqs 1 and 3.

Cell Surface Characterization. As shown in Table 2, electrophoretic mobility u_E and contact angles of bacteria

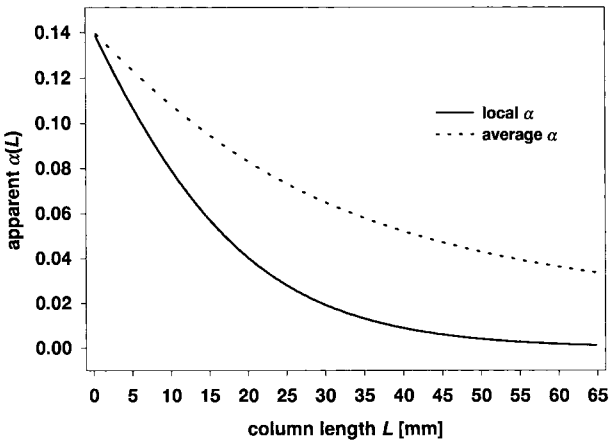

FIGURE 3. Apparent collision efficiencies α vs column length L as calculated based on eq 3 with the parameters derived from Figure 2 ($f_{fast} = 0.36$, $\alpha_{fast} = 0.32$, $\alpha_{slow} = 0.0032$). Curves show local α(L) and average α in columns of length L. The latter value for α is obtained when measured C/C_0 data for various L are interpreted in terms of filtration theory according to eq 1.

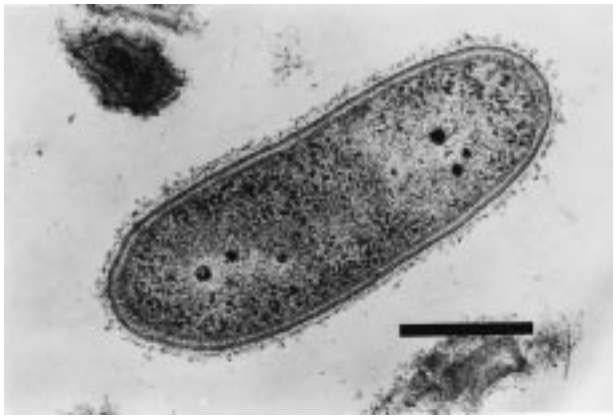

FIGURE 4. Electron micrograph of *Pseudomonas* sp. strain B13 after freeze substitution. On the cell body bounded by the two membrane layers, a diffuse layer of condensed material is visible. The bar is 0.5 μm in length.

are in agreement with published data obtained with other media (*28*). In contrast to other investigators (*42*), we did not find any variation during the life cycle. The isoelectric point reported at pH = 2.2 indicates the presence of cell surface polysaccharides (*43*). Electron micrographs revealed the presence of condensed material on the cell surface (Figure 4). This layer extended 20−50 nm into the medium and contained high amounts of LPS as shown by direct isolation. We purified the O-antigens, which are the part of the LPS actually reaching into the medium, and found number-averaged and mass-averaged molecular weights of 16 and 18 kDa, respectively, corresponding to approximate chain lengths of 36 and 40 nm (*44*).

Discussion of the Proposed Model in Terms of the DLVO Theory of Colloid Stability. Figure 5 shows an estimate of the interaction energy ΔG^{DLVO} as a function of surface to surface distance h for a cell approaching a sand grain. Basically, the attractive Lifshitz−van der Waals attraction counteracts the electrostatic repulsion between the two negatively charged surfaces. For all the contributions to ΔG^{DLVO}, the outer membrane of the cells was used as a reference for the separation distance h. This definition certainly is somewhat arbitrary in the presence of LPS as the outer boundary of the cells is fuzzy. The error in the h-scale is likely to be well below the polymer length, however. For ΔG^{EL} this argument is supported by the fact that most of the

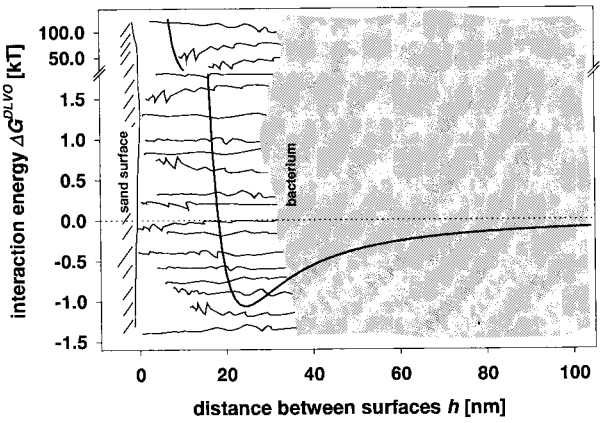

FIGURE 5. Interaction energy ΔG^{DLVO} vs separation distance h for a bacterium approaching a sand grain. The energy curve was estimated according to the DLVO theory of colloid stability with the parameters given in Table 1. An energy barrier of several hundred kT together with the lipopolysaccharides found on the cells are likely to keep them at least 20 nm from the sand surface. This indicates that deposition is governed by the secondary minima of the interaction energy curve.

negative charge of LPS is located close to the core region (*22*, *45*, *46*), and experiments with abiotic particles suggest that the shift is smaller than 10 nm in the presence of polymers (*20*). According to our calculations, a cell approaching a sand grain faces an energy barrier of several 100 kT due to electrostatic repulsion at $h \sim 20$ nm. In addition, comparison with the thickness of the LPS coating makes it immediately clear that many cells will be sterically hindered to reach such a close distance. We thus can restrict our reasoning to the secondary minimum region of $\Delta G^{DLVO}(h)$ on the solution side of the energy barrier.

Similar to ideas proposed by Marshall et al. (*47*), the deposition of bacteria could be rationalized in two steps: First, cells must have a kinetic energy smaller than the minimum in the interaction energy at the distance of closest possible approach (*48*−*50*). The collision efficiency α is then limited by the fraction of cells that satisfies this condition; all the others diffuse away from the surface immediately. But the cells remaining close to the collector are still subject to shear stress. A second step consisting in binding to the sand grains is thus required to keep them in place for a longer time.

The first step is determined by Brownian motion at low flow rates where the frequencies of the kinetic energies E_{kin} in the population $f(E_{kin})$ can be assumed to follow the Maxwell distribution (*51*):

$$f(E_{kin}) = \frac{2}{\sqrt{\pi} kT} \sqrt{\frac{E_{kin}}{kT}} \exp\left(-\frac{E_{kin}}{kT}\right) \quad (5)$$

Thus the upper limit of the collision efficiency might be derived from the depth of the secondary minimum in the interaction energy curve ΔG_{min}:

$$\alpha_{fast,th} = \int_0^{-\Delta G_{min}} f(E_{kin})\, dE = 1 - \int_{-\Delta G_{min}}^{\infty} f(E_{kin})\, dE \quad (6)$$

In our calculations, we found a minimum in $\Delta G^{DLVO}(h)$ at $h_{min} = 29$ nm with $\Delta G_{min} = -0.8kT$, resulting in a theoretical collision efficiency $\alpha_{fast,th} = 0.34$. For cells carrying a lot of LPS chains longer than h_{min}, ΔG at the distance of closest possible approach will be smaller in magnitude than ΔG_{min}, thus leading to a decrease of α_{fast}. Our experimental estimate $\alpha_{fast} = 0.32$ as derived from C/C_0 data seems thus in reasonable agreement with the predictions.

We propose that the discrimination between the two subpopulations f_{fast} and f_{slow} would occur in the second step. Only the ability of the cells in the fraction f_{fast} to anchor themselves fast enough to the sand grains makes them adhere with a collision efficiency α_{fast}. We think that the LPS molecules on the cell surface are responsible for this anchoring. Many authors suggested that surface polymers such as LPS played an important role in bacterial adhesion (*30*). Their molecular dimensions result in small colloidal forces. Hence, they are not subject to repulsion to the same extent as entire bacteria are, and they can contact a mineral surface. Once in close contact, LPS were shown to form hydrogen bonds with a binding energy of approximately 2.5kT each (*22*). If only a small portion of all the LPS molecules on a bacterium formed hydrogen bonds, the resulting binding energy would be high enough to anchor the cell. That this mechanism could indeed lead to deposition of cells is supported by interference reflection microscopy showing that bacteria may be attached while remaining at distances of up to 100 nm from the surface (*52*).

We hypothesize that the LPS of the fraction of cells f_{slow} with the low collision efficiency α_{slow} does not allow for immediate anchoring. Although their kinetic energy is low enough to prevent immediate escape, they are expected to be easily driven toward the bulk suspension. As a consequence, α_{slow} has to be smaller than α_{fast}. The residence time of these cells close to the energy minimum is suggested to depend on numerous factors, e.g. the time needed to diffuse out of the diffusion boundary layer (*26*), hydrodynamic shear forces and collision frequencies with other cells (*14*, *15*). Elimelech and O'Melia (*31*) summarize theoretical considerations predicting that, in the case of secondary minimum deposition, particles trapped near the surface but not immobilized are driven to the rear stagnation point of the collector (*31*). As several particles reach this point, they start expelling each other out of the minimum again. This results in a reversible kinetic process, and α_{slow} would no longer remain constant over time (*50*).

To date, the differences within the microbial population leading to the observed heterogeneity in the deposition remain unknown. Considering the tentative role of LPS in cell adhesion, either a varying average LPS length or variations in LPS composition leading to heterogeneous physicochemical properties are possible explanations (*46*).

Effect of Darcy Velocity U on C/C_0. For $U > 1$ cm h^{-1} the observed C/C_0 were in good agreement with predictions based on eqs 2 and 3 with the parameters calibrated to the $C(L)$ data of Figure 2 (Figure 6). For lower flow velocities, however, where the fraction of cells f_{fast} filtering with α_{fast} is entirely removed during column passage, deposition was underestimated. This implies that the collision efficiency α_{slow} of the slow deposition increases with a decreasing flow velocity and gradually exceeds the upper limit obtained from Figure 2 where $\alpha_{slow} < 10^{-2} \times \alpha_{fast}$. This seems plausible given the cumulative effects of decreasing shear forces and increasing thickness of the diffusion boundary layer as mentioned above. Furthermore, the validity of the approximations used to calculate η remains uncertain for low flow rates (*26*). The calculation of the theoretical removal is thus subjected to increasing uncertainty at low flow velocities.

The critical role of the flow velocity is further illustrated by a comparison with other deposition data obtained with *Pseudomonas* sp. strain B13. Rijnaarts et al. attributed its poor adhesion to glass or Teflon under static conditions in batch as well as in columns to steric hindrance resulting in a low α (*30*) or blocking (*10*), respectively. As U in our experiments was approximately 20 times lower, we observed improved removal in agreement with colloid filtration theory following eq 2. Only the use of these conditions allowed us to derive the model we propose.

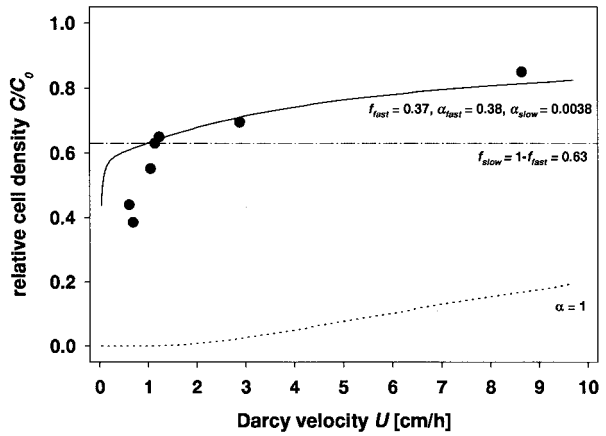

FIGURE 6. Relative cell density C/C_0 in the column outlet after initial breakthrough (2 pore volumes < t^* < 4 pore volumes) as a function of Darcy velocity U at an ionic strength of I = 8 mM. A theoretical curve obtained from eq 3 with the parameters derived from Figure 2 (—, f_{fast} = 0.36, α_{fast} = 0.32, α_{slow} = 0.0032) is in agreement with the experimental data as long as deposition is dominated by f_{fast} and α_{fast} ($C/C_0 > f_{slow}$). For slower flow, however, where C/C_0 depends on f_{slow} and α_{slow}, deposition is underestimated. A curve describing favorable deposition according to the colloid filtration theory with the parameters given in Table 1 is shown for comparison (- -).

Implications for the Transport of Microbes in Porous Media. Apart from hydrodynamic heterogeneity in aquifers, intra-population variability may result in surprisingly high microbial travel distances in the subsurface. Additionally, extrapolations are uncertain since a change in flow parameters might lead to a different deposition regime as we showed for the flow velocity. The colloid filtration theory as well as the DLVO theory of colloid stability provide valuable frameworks for assessing transport of bacteria in aquifers, but interpretations should be subject to careful verification.

Acknowledgments

We thank Ernst Wehrli (Laboratory for Electron Microscopy, ETH Zürich, Switzerland) for providing electron micrographs and Anja Sinke (TNO, Apeldoorn, The Netherlands) as well as Daniel Kobler (EAWAG, Dübendorf, Switzerland) for supplying the grain size analysis of the sand. Barbara Jucker (EAWAG) is acknowledged for helpful discussions. We are grateful to Menachem Elimelech (University of California, Los Angeles, CA) for his stimulating interest and critical review of the manuscript.

Literature Cited

(1) Bitton, G.; Gerba, C. In *Groundwater Pollution Microbiology*: *The Emerging Issue*; Bitton, G., Gerba, C. P., Eds.; John Wiley & Sons: New York, 1984; pp 1−7.
(2) Lawrence, J. R.; Hendry, M. J. *Can. J. Microbiol.* **1996**, *42*, 410−422.
(3) Rahe, T. M.; Hagedorn, C.; McCoy, E. L. *Water Air Soil Pollut.* **1978**, *11*, 93−103.
(4) Smith, M. S.; Thomas, G. W.; White, R. E.; Ritonga, D. *J. Environ. Qual.* **1985**, *14*, 87−91.
(5) Shales, S. W.; Kumarasingham, S. *J. Ind. Microbiol.* **1987**, *2*, 219−227.
(6) Martin, R. E.; Bouwer, E. J.; Hanna, L. M. *Environ. Sci. Technol.* **1992**, *26*, 1053−1058.
(7) Harvey, R. W.; Garabedian, S. P. *Environ. Sci. Technol.* **1991**, *25*, 178−185.
(8) Lindqvist, R.; Bengtsson, G. *Microb. Ecol.* **1991**, *21*, 49−72.
(9) Lindqvist, R.; Cho, J. S.; Enfield, C. G. *Water Resour. Res.* **1994**, *30*, 3291−3299.
(10) Rijnaarts, H. H. M.; Norde, W.; Bouwer, E. J.; Lyklema, J.; Zehnder, A. J. B. *Environ. Sci. Technol.* **1996**, *30*, 2877−2883.
(11) O'Melia, C. R. *Colloid Surf.* **1989**, *39*, 255−271.
(12) Albinger, O.; Biessemeyer, B. K.; Arnold, R. G.; Logan, B. E. *FEMS Microbiol. Lett.* **1994**, *124*, 321−326.
(13) Johnson, W. P.; Blue, K. A.; Logan, B. E.; Arnold, R. G. *Water Resour. Res.* **1995**, *31*, 2649−2658.
(14) Meinders, J. M.; van der Mei, H. C.; Busscher, H. J. *J. Colloid Interface Sci.* **1995**, *176*, 329−341.
(15) van de Ven, T. G. M. *Colloid Surf.* **1989**, *39*, 107−126.
(16) Dorn, E.; Hellwig, M.; Reineke, W.; Knackmuss, H.-J. *Arch. Microbiol.* **1974**, *99*, 61−70.
(17) Tros, M. E.; Schraa, G.; Zehnder, A. J. B. *Appl. Environ. Microbiol.* **1996**, *62*, 437−442.
(18) Adler, J. *J. Gen. Microbiol.* **1973**, *74*, 77−91.
(19) Stumm, W.; Morgan, J. J. *Aquatic Chemistry*, 3rd ed.; John Wiley & Sons: New York, 1996.
(20) Hunter, R. J. *Zeta potential in colloid science*; Academic Press: London, 1981.
(21) van Loosdrecht, M. C. M.; Norde, W.; Zehnder, A. J. B. *Appl. Environ. Microbiol.* **1987**, *53*, 1893−1897.
(22) Jucker, B.; Harms, H.; Hug, S. J.; Zehnder, A. J. B. *Colloid Surf. B* **1997**, *9*, 331−343.
(23) Müller, M.; Meister, N.; Moor, H. *Mikroskopie* **1980**, *36*, 129−140.
(24) Hohenberg, H.; Mannweiler, K.; Müller, M. *J. Microsc.* **1994**, *175*, 34−43.
(25) Reynolds, E. W. *J. Cell Biol.* **1963**, *17*, 208−212.
(26) Ryan, J. N.; Elimelech, M. *Colloid Surf. A* **1996**, *107*, 1−56.
(27) Logan, B. E.; Jewett, D. G.; Arnold, R. G.; Bouwer, E. J.; O'Melia, C. R. *J. Environ. Eng.* **1995**, *121*, 869−873.
(28) Rijnaarts, H. H. M.; Norde, W.; Bouwer, E. J.; Lyklema, J.; Zehnder, A. J. B. *Appl. Environ. Microbiol.* **1993**, *59*, 3255−3265.
(29) Bouwer, E. J.; Rittmann, B. E. *Environ. Sci. Technol.* **1992**, *26*, 400−401.
(30) Rijnaarts, H. H. M.; Norde, W.; Bouwer, E. J.; Lyklema, J.; Zehnder, A. J. B. *Colloid Surf. B* **1995**, *4*, 5−22.
(31) Elimelech, M.; O'Melia, C. R. *Langmuir* **1990**, *6*, 1153−1163.
(32) van Oss, C. J. *Interfacial forces in aqueous media*; Marcel Dekker: New York, 1994.
(33) van Loosdrecht, M. C. M.; Lyklema, J.; Norde, W.; Zehnder, A. J. B. *Microb. Ecol.* **1989**, *17*, 1−15.
(34) Gannon, J.; Tan, Y.; Baveye, P.; Alexander, M. *Appl. Environ. Microbiol.* **1991**, *57*, 2497−2501.
(35) Roy, S. B.; Dzombak, D. A. *Colloid Surf. A* **1996**, *119*, 133−139.
(36) Neu, T. R.; Marshall, K. C. *J. Biomater. Appl.* **1990**, *5*, 107−133.
(37) Gannon, J. T.; Manilal, V. B.; Alexander, M. *Appl. Environ. Microbiol.* **1991**, *57*, 190−193.
(38) Weiss, T. H.; Mills, A. L.; Hornberger, G. M.; Herman, J. S. *Environ. Sci. Technol.* **1995**, *29*, 1737−1740.
(39) Gross, M. J.; Logan, B. E. *Appl. Environ. Microbiol.* **1995**, *61*, 1750−1756.
(40) Jewett, D. G.; Hilbert, T. A.; Logan, B. E.; Arnold, R. G.; Bales, R. C. *Water Resour. Res.* **1995**, *29*, 1673−1680.
(41) McCaulou, D. R.; Bales, R. C.; McCarthy, J. F. *J. Contam. Hydrol.* **1994**, *15*, 1−14.
(42) Grasso, D.; Smets, B. F.; Strevett, D. A.; Machinist, B. D.; van Oss, C. J.; Giese, R. F.; Wu, W. *Environ. Sci. Technol.* **1996**, *30*, 3604−3608.
(43) Rijnaarts, H. H. M.; Norde, W.; Lyklema, J.; Zehnder, A. J. B. *Colloid Surf. B* **1995**, *4*, 191−197.
(44) Kastowsky, M.; Gutberlet, T.; Bradaczek, H. *J. Bacteriol.* **1992**, *174*, 4798−4806.
(45) Ferris, F. G.; Beveridge, T. J. *Can. J. Microbiol.* **1986**, *32*, 52−55.
(46) Makin, S. A.; Beveridge, T. J. *Microbiology* **1996**, *142*, 299−307.
(47) Marshall, K. C.; Stout, R.; Mitchell, R. *J. Gen. Microbiol.* **1971**, *68*, 337−348.
(48) Hogg, R.; Yang, K. C. *J. Colloid Interface Sci.* **1976**, *56*, 573−576.
(49) Marmur, A. *J. Colloid Interface Sci.* **1979**, *72*, 41−48.
(50) Hahn, M. W.; O'Melia, C. R., *Langmuir*, submitted for publication.
(51) Gehrtsen, C.; Kneser, H. O.; Vogel, H. *Physik*, 15th ed.; Springer: Berlin, 1989.
(52) Fletcher, M. *J. Bacteriol.* **1988**, *170*, 2027−2030.

Received for review October 23, 1997. Revised manuscript received April 7, 1998. Accepted April 16, 1998.

ES970936G